AJNR

This information is current as of June 1, 2023.

Intracranial stenoocclusive disease: MR angiography with magnetization transfer and variable flip angle.

G Fürst, M Hofer, H Steinmetz, J Kambergs, C Paselk, D Liebsch, A Aulich and U Mödder

Intracranial Stenoocclusive Disease: MR Angiography with Magnetization Transfer and Variable Flip Angle

Gü nter Fü rst, Matthias Hofer, Helmuth Steinmetz, Jö rg Kambergs, Christoph Paselk, Dietrich Liebsch, Albrecht Aulich, and Ulrich Mö dder

PURPOSE: To assess time-of-flight MR angiography that uses magnetization transfer contrast (MTC) pulses, tilted optimized nonsaturating excitation (TONE), and a 256×512 image matrix for the detection of small intracranial arteries and for the detection and quantification of intracranial arterial stenoocclusive disease. **METHODS:** To assess anatomic sensitivity, six interpreters, in a blinded fashion, reviewed the MTC/TONE MR angiograms and selective intraarterial angiograms obtained in 70 patients within a mean interval of 5.5 days (SD, 1.5). In addition, all intracranial angiograms were evaluated with regard to presence and degree of arterial stenosis and anatomic variants. **RESULTS:** Interobserver correlations for determining vessel length were comparably high for both methods. A strong correlation was found between measurements obtained on MR angiograms and those obtained on intraarterial angiograms. The mean vascular length averaged across all arteries was 34.8 mm (SD, 28.1) on MR angiograms and 53.2 mm (SD, 36.8) on intraarterial angiograms. Forty-one stenoses and occlusions and 30 anatomic variants were identified with intraarterial angiography. All arterial variants and 100% of occluded vessels were graded correctly. Moreover, 80% of stenoses greater than 70% and 88% of stenoses less than 70% were quantified correctly at MR angiography. Specificity for identifying stenotic disease was 99%. **CONCLUSION:** Despite inferior display of vessel length, MTC/TONE MR angiography with increased spatial resolution was able to show the vast majority of high-grade lesions visible at selective intraarterial angiography and may suffice for clinical decision making in many patients.

Index terms: Arteries, stenosis and occlusion; Arteries, magnetic resonance; Magnetic resonance angiography

The quality of time-of-flight magnetic resonance (MR) angiograms of the intracranial brain-supplying arteries can suffer from reduced signal caused by spin saturation, poor background suppression, and insufficient depiction of vascular detail. Recently, spatially variable flip angles have been shown to increase efficiently the signal on MR angiograms (1). Also, magnetization transfer contrast (MTC) pulses have been used to diminish signal from stationary tissue in brain and to improve substantially small-vessel depiction on maximum intensity projection (MIP) images (2). A previous study has shown that the combination of MTC and a variable flip angle produced the best overall MR angiographic quality for intracranial vessels (1). The objective of this prospective study was to assess the feasibility of time-of-flight MR angiography by using increased spatial resolution, a variable flip angle, and MTC pulses to depict the normal intracranial vasculature, detect anatomic variants, and quantify stenoocclusive disease.

Subjects and Methods

Patients

Seventy consecutive patients (39 male and 31 female; 1 month to 69 years old; median, 47 years) who had had

a retinal or cerebral transient ischemic attack or minor ischemic stroke were examined prospectively. Five of the patients were less than 12 years old. All patients were scheduled to undergo intraarterial and MR angiography of the intracranial arteries. Informed consent was obtained before each examination, and the mean interval between intraarterial and MR angiography was 5.5 days (SD, 1.5).

MR Angiography

All patients underwent arterial MR angiography on a 1.5-T whole-body scanner equipped with a circularly polarized head coil as receiver and transmitter. A three-dimensional gradient-echo fast imaging technique with steady-state precession and first-order flow compensation along the section- and frequency-encoding gradients was used (3). Technical parameters were 43/8 (repetition time/echo time), 52-mm slab thickness, 0.812-mm effective section thickness (64 partitions/slab), 200-mm field of view, and 256 × 512 image matrix. A variable flip angle radio-frequency pulse varied the slab excitation linearly from 10° to 30°. The effective flip angle at the center of the slab was 20° (nominal flip angle). The MTC pulse in this study was gaussian-shaped, 8.192 milliseconds in duration, and was applied 1.5 kHz off-resonance, with a bandwidth of 250 Hz. We investigated two or three image volumes overlapping by 20 partitions, covering the vascular system between the atlas loops of the vertebral arteries and the first segment of the callosomarginal arteries in patients with neurologic symptoms referable to the brain stem or cerebellum. In all other patients the MR angiographic slabs included the carotid siphon and the callosomarginal artery. A venous presaturation pulse was applied superiorly to the slab in all cases. Selective MR angiography was performed in nine patients using one or two arterial presaturation slabs (4). Angiographic projection images were reconstructed using an MIP algorithm (5). Additionally, targeted MIPs were used for anatomic evaluation (see below) to minimize vessel overlay and to reduce background noise (6). Eight images obtained in steps of 20° around a vertical and transverse axis of rotation were used for final evaluation.

Intraarterial Angiography

Selective digital subtraction intraarterial angiography of at least one carotid system and at least one vertebral system was carried out in all patients (103 carotid arteries, 82 vertebral arteries) using a 512 × 512 matrix and a 23-cm-diameter image intensifier. A minimum of two projections per arterial system allowed the delineation of the intracranial carotid artery, anterior, middle, and posterior cerebral arteries, and the vertebral and basilar arteries.

Evaluation and Data Analysis

MR angiograms and intraarterial angiograms were reviewed independently by six radiologists (three for each method). Pearson correlation coefficients were calculated to compare the results among readers (7).

Visibility of Vascular Detail

To assess anatomic sensitivity, the visibility (yes/no) of the following supratentorial and infratentorial arteries was noted by each reader: frontopolar artery, angular artery, posterior cerebral artery, posterior temporal artery, superior cerebellar artery, anterior inferior cerebellar artery, and posterior inferior cerebellar artery. If consensus could not be reached about whether an artery was visible, it was reported as not visible. For quantitative evaluation, the lengths of the above arteries were determined on lateral MR and intraarterial angiograms by using a map measurer. The arterial length was determined from the vessel origin to its end as seen on corresponding MR and intraarterial projection angiograms. If several terminal branches were visible, the longest branch was evaluated. MIP was targeted to the right and left hemispheres. Because vascular lengths cannot be measured directly on digital subtraction angiograms, all measurements were scaled to the length of the basilar artery as derived from the transverse single partitions of the MR angiographic data set.

Stenosis Quantification

The severity of intracranial stenosis was determined as the percentage of diameter reduction ($[1 - DS/DN] \times 100$) on the view showing the greatest extent of luminal narrowing. For this purpose, the minimum residual diameter (DS) and the nearby normal vessel diameter (DN) were measured by using a precision scale magnifier marked in tenths of a millimeter. Stenotic lesions were graded by each observer as mild (<30% reduction in diameter), moderate (30% to 69% reduction in diameter), severe (70% to 99% reduction in diameter), or occluded. In case of segmental signal void, the stenosis was graded as severe (>70%). If the reviewers disagreed, the higher grade of stenosis was recorded.

Results

Normal Vascular Anatomy

As compared with intraarterial angiography, in the supratentorial compartment, MR angiography showed the frontopolar arteries in 88% of cases, the angular arteries in 99%, the posterior cerebral arteries in 98%, and the posterior temporal arteries in 97% (Table 1). Infratentorially, 98% of the superior cerebellar arteries and 91% of the posterior inferior cerebellar arteries were visible at MR angiography. The greatest disagreement between readers occurred in regard to the anterior inferior cerebellar artery. Here, 18 (30%) of 61 anterior inferior cerebellar arteries seen on intraarterial angiograms were not

TABLE 1: Visibility of intracranial arteries and anatomic variants

Artery*	No. of Arteries Seen with Intraarterial Angiography	No. of Arteries Seen with both MR Angiography and Intraarterial Angiography	No. of Arteries Seen with MR Angiography Alone
Frontopolar (91)	81	71	0
Angular (103)	97	96	0
Posterior cerebral (106)	96	94	0
Posterior temporal (106)	93	90	0
Superior cerebellar (108)	98	96	1
AICA (102)	61	43	6
PICA (74)	67	61	0
Fetal posterior cerebral	18	18	0
A1: aplasia/hypoplasia	6	6	0
Vertebral terminating as PICA	5	5	0
Carotid-basilar anastomosis	1	1	0

Note.—AICA indicates anterior inferior cerebellar artery; PICA, posterior inferior cerebellar artery.

* Numbers in parentheses are numbers of vascular territories evaluated with intraarterial and MR angiography. Note that numbers in column 1 are different from those in columns 2 and 3, indicating lack of visibility due to occlusion, aplasia, or technical limitations. Note also that numbers of superior cerebellar arteries, AICAs, and PICAs evaluated are different, as intraarterial and MR angiography did not include all intracranial arteries in all patients, depending on the clinical indication.

TABLE 2: Lengths of intracranial arteries

Artery	Mean Length, mm (SD)			P Value
	MR Angiography	Intraarterial Angiography	Difference	
Frontopolar	33.7	40.0	6.3	
	(18.6)	(15.8)	(16.1)	<.05
Angular	77.9	108.7	30.8	
	(23.3)	(26.7)	(16.7)	<.0001
Posterior cerebral	48.6	64.6	16.0	
	(19.7)	(23.0)	(17.2)	<.0005
Posterior temporal	31.1	43.4	12.3	
	(16.6)	(17.8)	(16.3)	<.0008
Superior cerebellar	32.4	39.1	6.7	
	(15.3)	(19.5)	(17.4)	<.05
AICA	16.5	18.1	1.6	
	(14.7)	(19.0)	(14.7)	>.05
PICA	35.1	48.2	13.1	
	(18.7)	(31.5)	(21.5)	<.01

Note.—AICA indicates anterior inferior cerebellar artery; PICA, posterior inferior cerebellar artery.

unanimously identified on MR angiograms. MR angiographic measurements of arterial lengths correlated strongly with independent measurements based on intraarterial angiography (r = .81; $P <$ .0001) (Table 2). Interobserver correlations (Pearson correlation coefficients) for determining arterial lengths ranged from 0.96 to 0.97 (median, 0.96) for MR angiography and from 0.91 to 0.95 (median, 0.93) for intraarterial angiography. The mean length averaged across all arteries and patients was 34.8 mm (SD, 28.1) for MR angiography and 53.2 mm (SD, 36.8) for intraarterial angiography. The difference between MR angiography and in-

traarterial angiography was statistically significant ($P <$ .05) for all arteries, except for the anterior inferior cerebellar artery ($P >$ .05) (Table 2).

Anatomic Variants and Collateral Flow

Hypoplasia or aplasia of the horizontal (A1) segment of the anterior cerebral artery at intraarterial angiography was seen in six carotid territories and corresponded to narrow luminal size or invisibility of this arterial segment at MR angiography (Fig 1). There was no false-negative MR angiographic result concerning the

presence of an A1 segment. All 14 subjects with unilateral and two patients with bilateral fetal origin of the posterior cerebral artery from the internal carotid artery were correctly identified at MR angiography. A carotid-basilar anastomosis was seen in one patient, and a vertebral artery ending as the posterior inferior cerebellar artery was seen in five patients. Cross flow via the anterior communicating artery was recognized at selective MR angiography in four patients with high-grade stenosis or occlusion of the extracranial carotid artery. Collateral flow via the posterior communicating artery was cor-

rectly depicted in three patients with ipsilateral extracranial high-grade internal carotid artery stenosis (posterior to anterior collateral flow), and in one patient with high-grade stenosis of the basilar artery (anterior to posterior flow) (Fig 2). There were no false-negative or false-positive results.

Stenoocclusive Disease

A total of 417 normal intracranial arteries and 41 intracranial stenoses and occlusions were available for review (Table 3). Five arteries were
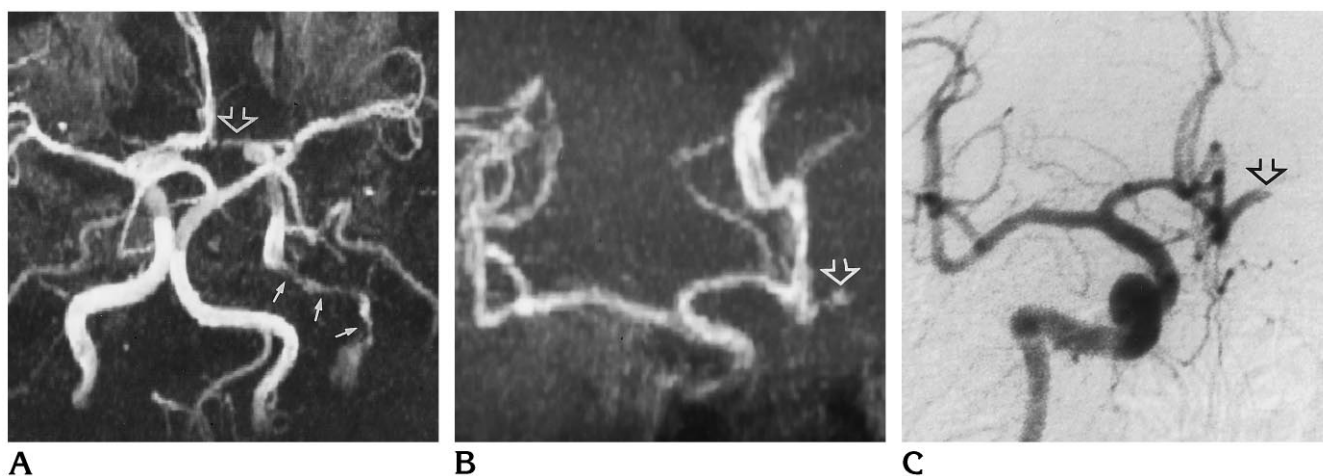

Fig 1. Nonselective MR angiogram (*A*), selective MR angiogram (*B*), and intraarterial angiogram (*C*) of the right carotid artery in a patient with high-grade luminal narrowing of the left extracranial internal carotid artery resulting from dissection (*A*, view from below; *B* and *C*, frontal views). The extracranial stenosis (not shown) extends into the petrous portion of the carotid artery (*solid arrows* in *A*). Selective MR angiogram and intraarterial angiogram (*B* and *C*) show no right-to-left collateral flow due to hypoplasia of the horizontal portion (A1) of the left anterior cerebral artery (*open arrow*). Selective MR angiogram (*B*) was obtained using selective presaturation of the left carotid and both vertebral arteries.
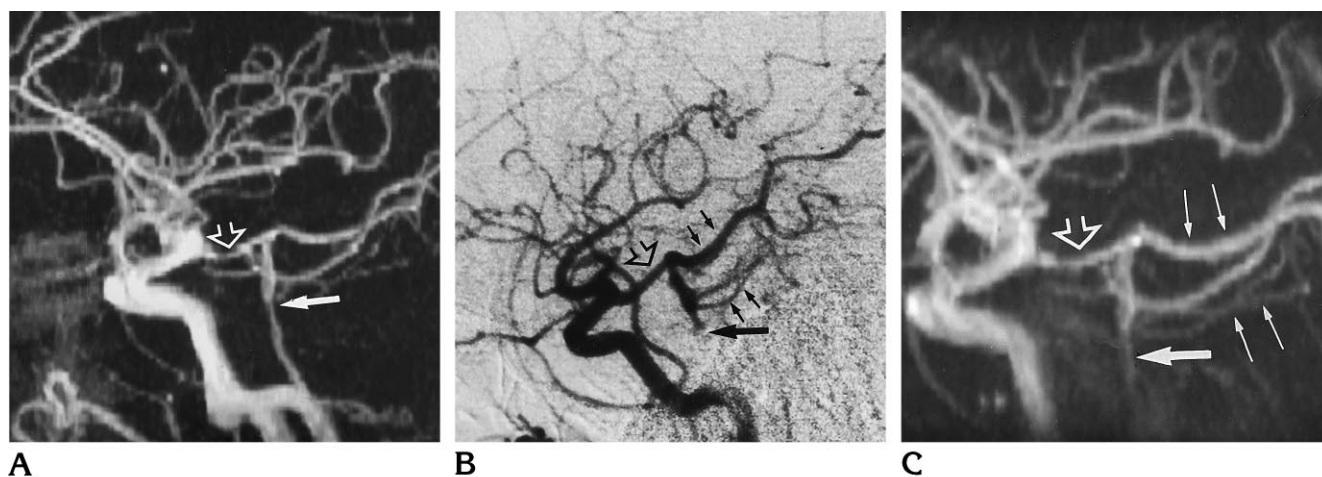

Fig 2. Nonselective MR angiogram (*A*) in a patient with high-grade stenosis (>70%) of the basilar artery (*solid arrow*). Selective intraarterial (*B*) and MR (*C*) angiograms of the left carotid artery show collateral flow via the posterior communicating artery (*open arrow*) into the basilar, posterior cerebral, and superior cerebellar arteries (*small arrows*) (*A–C*, lateral views). Selective MR angiography was performed using selective presaturation of the vertebral arteries and the right carotid artery.

TABLE 3: Quantification of intracranial arterial disease with MR angiography and intraarterial angiography in 70 patients

MR Angiography	Intraarterial Angiography				
	Normal	<30% Stenosis	30% to 69% Stenosis	70% to 99% Stenosis	Occlusion
Normal	414	. . .	. . .	1	. . .
<30% stenosis	. . .	1	. . .	. . .	. . .
30% to 69% stenosis	1	. . .	3	. . .	. . .
70% to 99% stenosis	2	1	. . .	14	. . .
Occlusion	. . .	. . .	. . .	1	20
Total	**417**	**2**	**3**	**16**	**20**

Note.—Total number of examined arteries was 458 (91 anterior, 103 middle, 106 posterior cerebral arteries; 103 internal carotid arteries; and 55 basilar arteries).
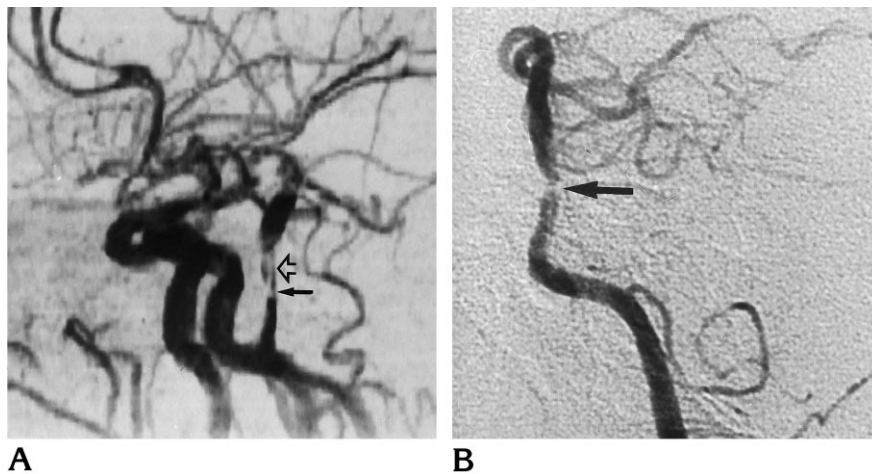

A   B

Fig 3. MR (*A*) and intraarterial (*B*) angiograms in a patient with high-grade (>70%) basilar artery stenosis (*solid arrow*) (*A* and *B*, lateral views). Note intraluminal signal loss distal to stenosis (*open arrow*).

graded as mildly or moderately stenosed (1% to 69%) (one carotid artery, two vertebral arteries, one basilar artery, and one middle cerebral artery). Sixteen arteries were severely narrowed (70% to 99%) (two carotid arteries, three basilar arteries, one vertebral artery, five middle cerebral arteries, two anterior cerebral arteries, and three posterior cerebral arteries) and 20 arteries were occluded (one carotid artery, six vertebral arteries, three basilar arteries, seven middle cerebral arteries, and three posterior cerebral arteries). Fourteen (88%) of 16 of the high-grade lesions (Figs 2–4) and all 20 (100%) of the occlusions (Fig 5) were correctly graded (Table 3). One severely stenotic middle cerebral artery was misinterpreted as occluded. A high between-method agreement was found for vessels with less than 70% luminal narrowing (Table 3). Three normal or mildly stenotic vessels were misinterpreted as severely stenotic.

Artifacts

Intrastenotic and poststenotic signal loss was observed in seven lesions with more than 70%

reduction in luminal diameter (one carotid artery, two basilar arteries, three middle cerebral arteries, and one posterior cerebral artery) (Figs 3 and 6). Twenty-one of 103 MR angiograms of the intracranial internal carotid and/or horizonal (M1) middle cerebral arteries were compromised by irregular signal. Four of these vessels were misinterpreted as more severely stenotic than they appeared at intraarterial angiography (Table 3). Conversely, the degree of luminal narrowing was underestimated in one carotid artery, because the readers misinterpreted the signal intensity loss as an artifact simulating stenosis (Table 3).

Discussion

In the present study, most of the supratentorial and infratentorial arteries were reliably and accurately recognized, thus providing valid information about whether a particular artery was occluded or patent. On average, arterial length measured with MR angiography was only 35% shorter than length determined with intraarterial angiography, suggesting the feasibility of MR
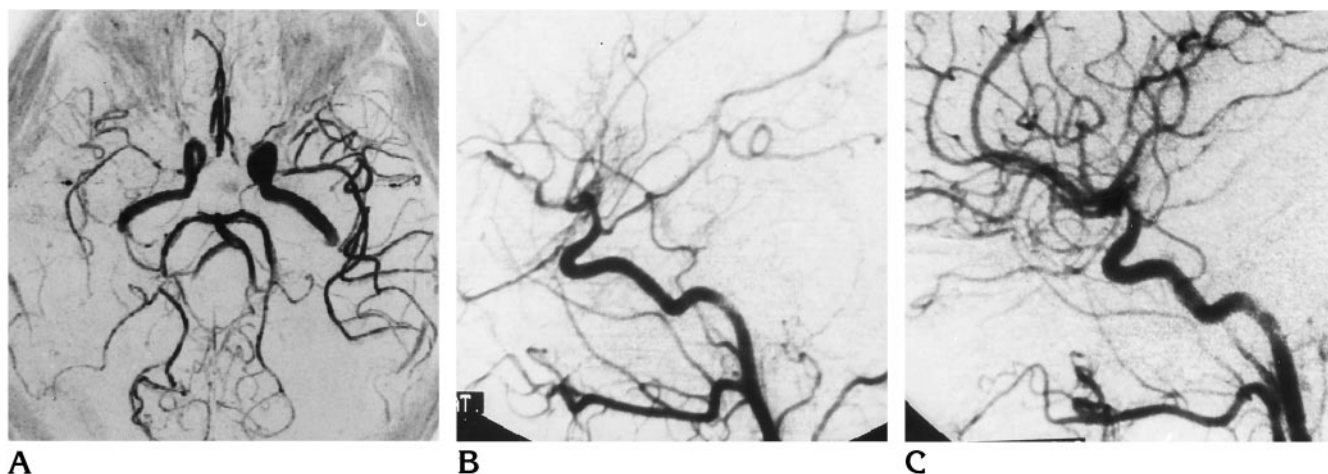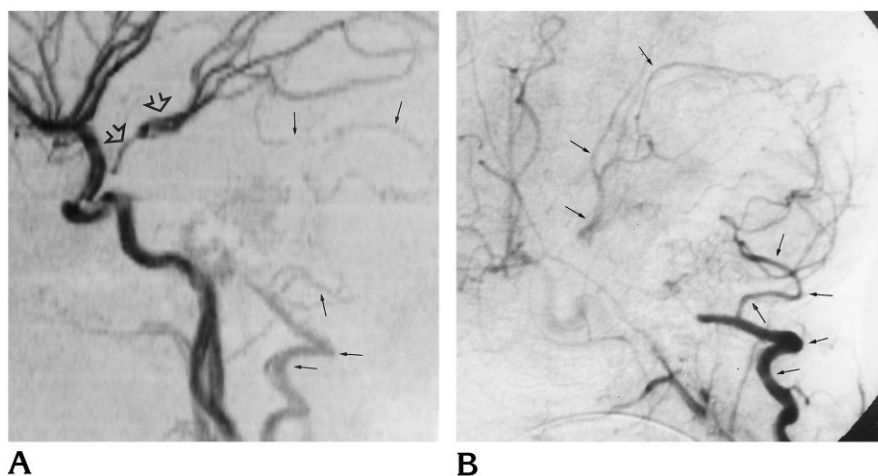
Fig 4. MR angiogram (*A*) and intraarterial angiograms of the right (*B*) and left (*C*) carotid territories. Both studies are of a patient with cerebral vasculitis (*A*, view from below; *B* and *C*, lateral views). MR angiogram (*A*) and intraarterial arteriogram (*B*) depict severe luminal narrowing of the right middle cerebral artery and its branches compared with the unaffected contralateral hemisphere (*A* and *C*).

Fig 5. Lateral MR (*A*) and intraarterial (*B*) angiograms of an 18-month-old child with recurrent cardiac embolism. Both angiograms depict a complete embolic occlusion of the basilar artery. The posterior cerebral arteries are supplied via posterior communicating arteries (*open arrows*). Note also collateral supply of the cerebellum via vertebral arteries, posterior inferior cerebellar arteries, and superior cerebellar arteries (*solid arrows*). MR tomography (not shown) revealed multiple infarcts in the brain stem but not in the cerebellum.

angiography as used here to depict all major brain-supplying intracranial arteries. In contrast, only 70% of the anterior inferior cerebellar arteries seen at intraarterial angiography were correctly identified at MR angiography. Nevertheless, compared with previous investigations by Wentz at al (8), who reported a detectability rate of only 50% for this vessel using a technique with poorer spatial and contrast resolution, these results indicate methodological improvement. In addition, our findings show that arterial variants can be reliably identified with MR angiography.

Until now, intraarterial angiography has been considered the standard of reference for detecting and quantifying intracranial arterial stenoses. However, several recent prospective studies showed that intraarterial angiography still

carries a 1% to 2% rate of cerebral infarction in patients with symptomatic cerebrovascular disease (9–12). Promising results for the identification and quantification of extracranial carotid stenoses with MR angiography have been described in several studies (13–19). The clinical experience with regard to intracranial stenoocclusive disease is still limited. Heiserman et al (20) studied the usefulness of MR angiography in detecting intracranial vascular disease in 29 patients. More recently, Korogi et al (21) and Wentz et al (8) reported relatively good sensitivities and specificities in distinguishing between normal and diseased intracranial arteries. However, these studies were limited to either the intracranial carotid and middle cerebral arteries (21) or the vertebrobasilar system (8). Moreover, the MR angiographic techniques used in
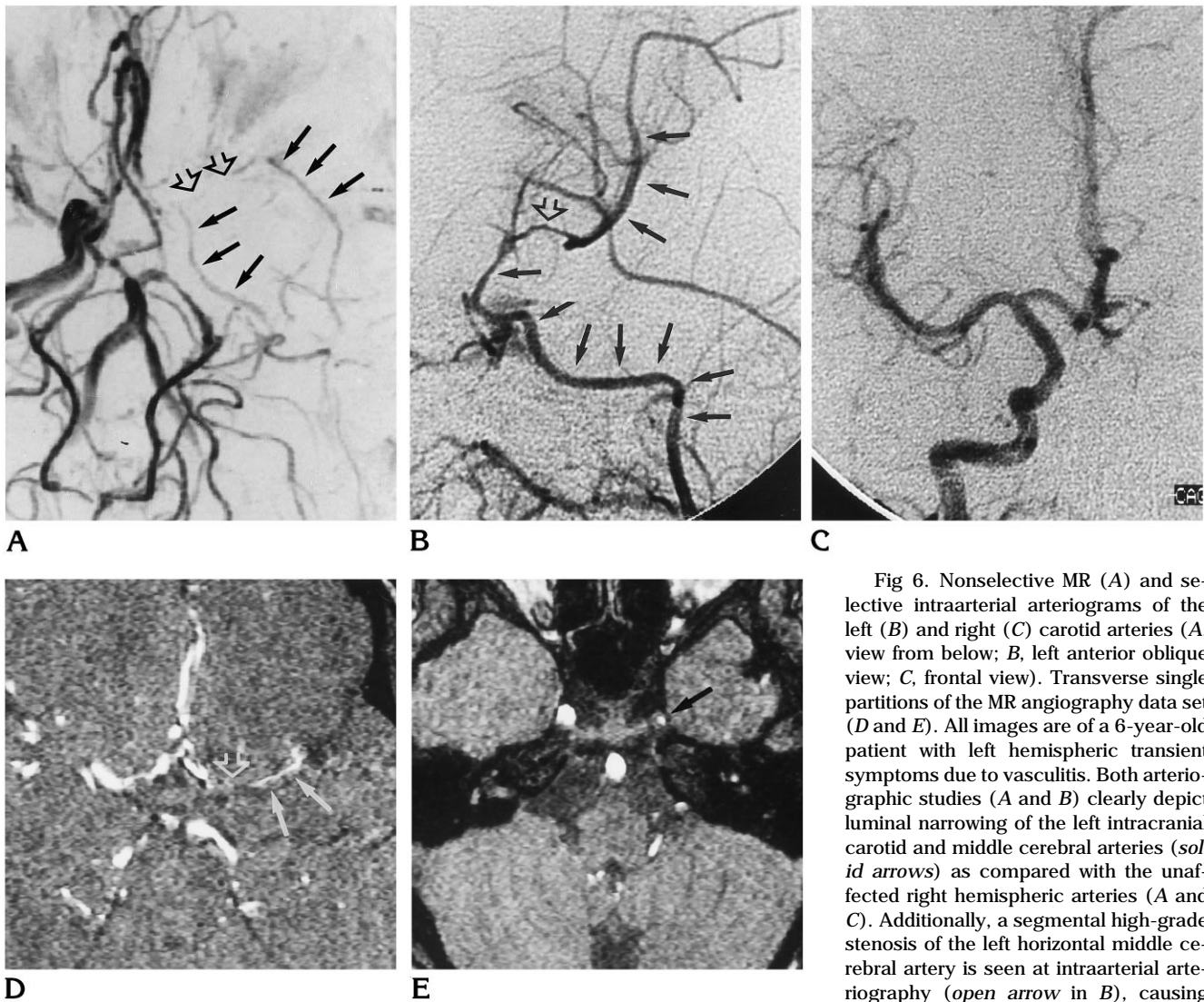
Fig 6. Nonselective MR (*A*) and selective intraarterial arteriograms of the left (*B*) and right (*C*) carotid arteries (*A*, view from below; *B*, left anterior oblique view; *C*, frontal view). Transverse single partitions of the MR angiography data set (*D* and *E*). All images are of a 6-year-old patient with left hemispheric transient symptoms due to vasculitis. Both arteriographic studies (*A* and *B*) clearly depict luminal narrowing of the left intracranial carotid and middle cerebral arteries (*solid arrows*) as compared with the unaffected right hemispheric arteries (*A* and *C*). Additionally, a segmental high-grade stenosis of the left horizontal middle cerebral artery is seen at intraarterial arteriography (*open arrow* in *B*), causing signal loss at MR angiography (*open arrows* in *A* and *D*). The MR angiographic source images also depict luminal narrowing of the middle (*D*) and internal carotid arteries (*E*) (*arrows*).

these studies provided relatively low spatial and contrast resolution. In the present investigation, 99% of normal and 100% of occluded vessels were correctly graded. Also, 80% of the less than 70% stenoses and 88% of the greater than 70% stenoses were classified accurately, indicating the feasibility of MTC/TONE MR angiography for detecting and quantifying intracranial arterial stenoocclusive disease. It deserves mentioning that such information has become of increasing clinical importance since the warfarin-aspirin symptomatic intracranial disease study suggested a considerable benefit of oral anticoagulation in patients with symptomatic high-grade intracranial arterial stenosis (22). That study found an approximately 50% reduc-

tion in stroke risk for patients being treated with warfarin as compared with aspirin.

As in previous investigations, artifactual signal loss represented the most relevant limitation of MR angiography in the present study, interfering with the identification and quantification of stenotic disease. With the use of three-dimensional time-of-flight techniques, signal loss may be relevant under different circumstances. Heiserman et al (20) emphasized that vessels lying near the sphenoidal sinus, especially the paracavernous and supraclinoid portions of the internal carotid arteries, are particularly subject to artifactual narrowing or lack of visibility caused by the large susceptibility gradients present in this area. In our series, 20% of the

intracranial MR angiograms were compromised by irregular or discontinuous signal intensity in vessels close to the skull base (internal carotid and proximal middle cerebral arteries). However, this circumstance led to misinterpretation of the degree of stenosis in only five vessels. Saturation of slow flow represents a second drawback of volume excitation and can falsely eliminate signal, especially downstream of a very tight stenosis. A false diagnosis of occlusion resulting from this phenomenon occurred in one high-grade stenosis of the horizontal middle cerebral artery. Owing to the directional sensitivity of time-of-flight methods, even such recent technical refinements as thin overlapping slabs and variable flip angle cannot eliminate this pitfall for flow in the in-plane direction. Third, current MR angiographic techniques have proved sensitive to signal void in areas of flow constriction and complex vascular anatomy (16, 19). The underlying mechanisms of flow-induced spin dephasing have been described by several authors (23–26). As in previous investigations of extracranial carotid stenosis (19), we observed intrastenotic and poststenotic signal loss in stenoses with greater than 70% luminal narrowing (n = 7) (Figs 3 and 6). Echo time was relatively long in our study (8 milliseconds). More efficient suppression of flow-induced signal loss would probably be achieved by shorter echo times, as has recently been demonstrated experimentally and clinically (27–30).

In conclusion, despite certain limitations MTC/TONE MR angiography with increased spatial resolution can provide reliable information about presence and degree of intracranial stenoocclusive disease. In addition, improved MR angiography may play a role in the acute work-up of patients with stroke and help to further reduce the number of invasive procedures.

Acknowledgment

References

1. Atkinson D, Brant-Zawadzki M, Gillan G, Purdy D, Laub G. Improved MR angiography: magnetization transfer suppression with variable flip angle excitation and increased resolution. *Radiology* 1994;190:890–894

2. Edelman RR, Ahn SS, Chien D, et al. Improved time-of-flight MR angiography of the brain with magnetization transfer contrast. *Radiology* 1992;184:395–399

3. Laub GA, Kaiser WA. MR angiography with gradient motion refocusing. *J Comput Assist Tomogr* 1988;12:377–382

4. Fü rst G, Steinmetz H, Fischer H, et al. Selective MR angiography in the evaluation of intracranial arterial collateral blood flow. *J Comput Assist Tomogr* 1993;17:178–183

5. Laub G. Displays for MR angiography. *Magn Reson Med* 1990;14:222–229

6. Anderson CM, Saloner D, Tsuruda JS, et al. Artifacts in maximum-intensity-projection display of MR angiograms. *AJR Am J Roentgenol* 1990;154:623–629

7. Altman DG. Relation between two continuous variables. In: *Practical Statistics for Medical Research.* Altman DG, ed. London, England: Chapman and Hall; 1992:277–299

8. Wentz KU, Rö ther J, Schwartz A, Mattle HP, Suchalla R, Edelman RR. Intracranial vertebrobasilar system: MR angiography. *Radiology* 1994;190:105–110

9. Executive Committee of the Asymptomatic Carotid Atherosclerosis Study. Endarterectomy for asymptomatic carotid artery stenosis. *JAMA* 1995;273:1421–1428

10. Earnest F, Forbes G, Sandok BA, et al. Complications of cerebral angiography: prospective assessment of risk. *AJNR Am J Neuroradiol* 1983;4:1191–1197

11. Dion JE, Gates PC, Fox AJ, Barnett HJM, Blom RJ. Clinical events following neuroangiography: a prospective study. *Stroke* 1987;18:997–1004

12. Davies KN, Humphrey PR. Complications of cerebral angiography in patients with symptomatic carotid territory ischemia screened by carotid ultrasound. *J Neurol Neurosurg Psychiatry* 1993;56:967–972

13. Anderson CM, Saloner D, Lee RE, et al. Assessment of carotid artery stenosis by MR angiography: comparison with x-ray angiography and color-coded Doppler ultrasound. *AJNR Am J Neuroradiol* 1992;13:989–1003

14. Litt AW, Eidelman EM, Pinto RS, et al. Diagnosis of carotid artery stenosis. *AJNR Am J Neuroradiol* 1991;12:149–154

15. Mattle HP, Kent KC, Edelman RR, Atkinson DJ, Skillman JJ. Evaluation of the extracranial carotid arteries: correlation of magnetic resonance angiography, duplex sonography, and conventional angiography. *J Vasc Surg* 1991;13:835–845

16. Polak JF, Bajakian RL, O'Leary DH, Anderson CM, Donaldson MC, Jolesz FA. Detection of internal carotid artery stenosis: comparison of MR angiography, color Doppler sonography, and angiography. *Radiology* 1992;182:35–40

17. Heiserman JE, Drayer BP, Fram EK, et al. Carotid artery stenosis: clinical efficacy of two-dimensional time-of-flight MR-angiography. *Radiology* 1992;182:761–768

18. Masaryk AM, Ross JS, DiCello MC, Modic MT, Paranandi l, Masaryk TJ. 3DFT MR angiography of the carotid bifurcation: potential and limitations as a screening examination. *Radiology* 1991;179:797–804

19. Sitzer M, Fü rst G, Fischer H, et al. Between-method correlation in quantifying internal carotid stenosis. *Stroke* 1993;24:1513–1518

20. Heiserman JE, Drayer BP, Keller PJ, Fram EK. Intracranial vascular stenosis and occlusion: evaluation with three-dimensional time-of-flight MR angiography. *Radiology* 1992;185:667–673

21. Korogi J, Takahashi M, Mabuchi N, et al. Intracranial vascular stenosis and occlusion: diagnostic accuracy of three-dimensional, Fourier transform time-of-flight MR angiography. *Radiology* 1994;193:187–193

22. Chimowitz MI, Kokkinos J, Strong J, et al. The warfarin-aspirin symptomatic intracranial disease study. *Neurology* 1995;45:1488–1493

23. Bradley WG, Waluch V, Lai KS, Fernandez EJ, Spalter C. The appearance of rapidly flowing blood on magnetic resonance images. *AJR Am J Roentgenol* 1984;143:1167
24. Evans A, Russell BA, Blinder A, et al. Effects of turbulence on signal intensity in gradient echo images. *Invest Radiol* 1988;23: 512–518
25. Von Schulthess GK, Higgins CB. Blood flow imaging with MR: spin phase phenomena. *Radiology* 1985;157:687
26. Urchuk SN, Plewes DB. Mechanisms of flow-induced signal loss in MR-angiography. *J Magn Reson Imaging* 1992;2:453–462
27. Fü rst G, Hofer M, Sitzer M, Kahn T, Mü ller E, Mö dder U. Factors influencing flow-induced signal loss in MR angiography: an in vitro study. *J Comput Assist Tomogr* 1995;19:692–699
28. Gatenby J, McCauley H, Gore J. Mechanisms of signal loss in magnetic resonance imaging of stenoses. *Med Phys* 1993;20: 1049–1056
29. Kilner PJ, Firmin DN, Rees RSO, et al. Valve and great vessel stenosis: assessment with MR jet velocity mapping. *Radiology* 1991;178:229–235
30. Lin W, Tkach JA, Haacke EM, Masaryk TJ. Intracranial MR angiography: application of magnetization transfer contrast and fat saturation to short gradient-echo, velocity-compensated sequences. *Radiology* 1993;186:753–761